Prompt photon associated with jet photoproduction at HERA in the parton Reggeization approach

B. A. Kniehl[1], M. A. Nefedov[1,2], V. A. Saleev[2]

ICHEP 2014
Valencia, Spain

[1] II. Institut für Theoretische Physik, Universität Hamburg
[2] Samara State University, Samara, Russia

Outline.

This talk is based on the results, published in [B. A. Kniehl, M. A. Nefedov, V. A. Saleev, Phys. Rev. D**89** 114016 (2014)]

1. Introduction to the parton Reggeization approach (PRA).
   - Motivation
   - Reggeization of the amplitudes
   - Effective action
   - Factorization formula and KMR unPDF
2. Prompt photon + jet photoproduction.
   - Photoproduction kinematics
   - Motivation of the present study
   - Subprocesses in the LO PRA
3. Tree-level contributions.
4. "Box" contribution ($\gamma R \to \gamma g$).
5. Numerical results.
6. Conclusion.

Motivation for k_T-factorization and PRA.

- The class of processes, suitable for the study in k_T-factorization is the *central* production of the final state of interest by the *small-x* ($x \lesssim 10^{-2} - 10^{-3}$) partons in the $pp(\bar{p})$ or ep collisions.
- In this kinematics, most of the initial state radiation is highly separated in rapidity from the central region, and can be factorized. In the small-x regime, initial state partons carry the substantial transverse momentum (virtuality) $|\mathbf{q}_T| \sim x\sqrt{S}$, in contrast with the standard Collinear Parton Model (CPM), where $|\mathbf{q}_T| \ll x\sqrt{S}$, and can be neglected. This is the standard setup of the k_T-*factorization* [L. V. Gribov *et. al.* 1983; J. C. Collins *et. al.* 1991; S. Catani *et. al.* 1991].
- The the gauge-invariant procedure to take into account the virtuality of the initial state parton (quark or gluon) in the amplitude of the hard scattering, is required.

In present time, three methods proposed to solve the last problem:

- The standard k_T-factorization prescription gluons ($\varepsilon^\mu(k) = \frac{k_T^\mu}{|\mathbf{k}_T|}$).
- The parton Reggeization approach (PRA).
- Methods based on the extraction of certain asymptotics of the amplitudes in the spinor-helicity representation (see e. g. [A. van Hameren *et. al.*, Phys.Lett. B727 226 (2013)]).

There is, in fact, a chain of succession between these three methods.

Reggeization of amplitudes in QCD.

PRA is based on the Reggeization of amplitudes in gauge theories (QED, QCD, Gravity). The *high energy asymptotics* of the $2 \to 2+n$ amplitude is dominated by the diagram with t-channel exchange of the effective (Reggeized) particle and Multi-Regge (MRK) or Quasi-Multi-Regge Kinematics (QMRK) of final state.

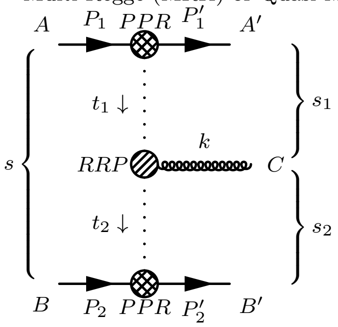

In the limit $s \to \infty$, $s_{1,2} \to \infty$, $-t_1 \ll s_1$, $-t_2 \ll s_2$ (Regge limit), $2 \to 3$ amplitude has the form:

$$\mathcal{A}_{AB}^{A'B'C} = 2s\gamma_{A'A}^{R_1} \left(\frac{s_1}{s_0}\right)^{\omega(t_1)} \frac{1}{t_1} \times$$

$$\times \Gamma_{R_1 R_2}^{C}(q_1, q_2) \times \frac{1}{t_2} \left(\frac{s_2}{s_0}\right)^{\omega(t_2)} \gamma_{B'B}^{R_2}$$

$\Gamma_{R_1 R_2}^{C}(q_1, q_2)$ - RRP effective production vertex,

$\gamma_{A'A}^{R}$ - PPR effective scattering vertex,

$\omega(t)$ - Regge trajectory.

Two approaches to obtain this asymptotics:

- BFKL-approach (Unitarity, renormalizability and gauge invariance), see [B. Ioffe, V. S. Fadin, L. N. Lipatov, QCD – Perturbative and Nonperturbative aspects].
- Effective action approach [L. N. Lipatov, Nucl. Phys. B**452** (1995) 369].

The field content of the effective theory.

Light-cone vectors:

$$n^{+} = \frac{2P_2}{\sqrt{S}},\ n^{-} = \frac{2P_1}{\sqrt{S}},\ n^{+}n^{-} = 2$$

$$x^{\pm} = n^{\pm}x = x^0 \pm x^3,\ \partial_{\pm} = 2\frac{\partial}{\partial x^{\mp}}$$

Lagrangian of the effective theory $L = L_{kin} + \sum_{y} \left(L_{QCD} + L_{ind}\right)$, $v_\mu = v_\mu^a t^a$, $\left[t^a, t^b\right] = f^{abc}t^c$. Each subinterval in rapidity $(1 \ll \eta \ll Y)$ has it's own set of QCD fields:

$$L_{QCD} = -\frac{1}{2} tr\left[G_{\mu\nu}^2\right],\ G_{\mu\nu} = \partial_\mu v_\nu - \partial_\nu v_\mu + g\left[v_\mu, v_\nu\right].$$

Different rapidity intervals communicate via Reggeized gluons $(A_{\pm} = A_{\pm}^a t^a)$ with the kinetic term:

$$L_{kin} = -\partial_\mu A_+^a \partial^\mu A_-^a,$$

and the kinematical constraint:

$$\partial_- A_+ = \partial_+ A_- = 0 \Rightarrow$$

$$A_+ \text{ has } k_- = 0 \text{ and } A_- \text{ has } k_+ = 0.$$

The effective action for high energy processes in QCD.

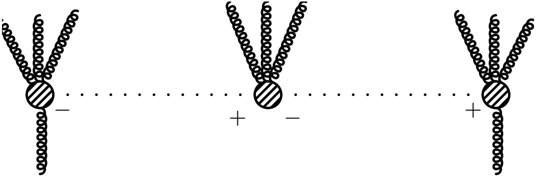

Particles and Reggeons interact via *induced interactions*:

$$L_{ind} = - tr\left\{ \frac{1}{g}\partial_+ \left[P\exp\left(-\frac{g}{2}\int\limits_{-\infty}^{x^-} dx'^- v_+(x') \right)\right] \cdot \partial_\sigma \partial^\sigma A_-(x) + \right.$$

$$\left. + \frac{1}{g}\partial_- \left[P\exp\left(-\frac{g}{2}\int\limits_{-\infty}^{x^+} dx'^+ v_-(x') \right)\right] \cdot \partial_\sigma \partial^\sigma A_+(x) \right\}$$

Wilson lines lead to the infinite chain of the induced vertices:

$$L_{ind} = tr\left\{ \left[v_+ - g v_+ \partial_+^{-1} v_+ + g^2 v_+ \partial_+^{-1} v_+ \partial_+^{-1} v_+ - \ldots \right] \partial_\sigma \partial^\sigma A_- + \right.$$

$$\left. + \left[v_- - g v_- \partial_+^{-1} v_- + g^2 v_- \partial_-^{-1} v_- \partial_-^{-1} v_- - \ldots \right] \partial_\sigma \partial^\sigma A_+ \right\}$$

Factorization of the cross-section.

Factorization:

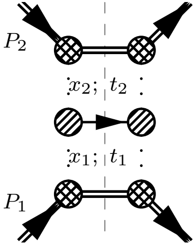

Factorization formula:

$$d\sigma = \int \frac{d^2\mathbf{q}_{T1}}{\pi} \int \frac{dx_1}{x_1} \Phi(x_1, t_1, \mu_F) \times$$
$$\times \int \frac{d^2\mathbf{q}_{T2}}{\pi} \int \frac{dx_2}{x_2} \Phi(x_2, t_2, \mu_F) d\hat{\sigma}_{PRA}$$

Where Φ - Unintegrated PDFs.

Partonic cross-section:

$$d\hat{\sigma}_{PRA} = \frac{(2\pi)^4}{2x_1x_2S} \overline{|\mathcal{M}|^2}_{PRA} \delta^{(4)}(P_{[i]} - P_{[f]}) \times$$
$$\times \prod_{j=[f]} \frac{d^3\mathbf{p}_j}{(2\pi)^3 2p_j^0},$$

Normalization of the unPDF:

$$\int^{\mu^2} dt \Phi(x, t, \mu^2) = xf(x, \mu^2),$$

where $f(x, \mu^2)$ - collinear PDF, implies, that the *collinear limit* holds for the amplitude:

$$\int \frac{d\phi_1 d\phi_2}{(2\pi)^2} \lim_{t_{1,2}\to 0} \overline{|\mathcal{M}|^2}_{PRA} = \overline{|\mathcal{M}|^2}_{CPM}$$

The Kimber-Martin-Ryskin unPDF.

Kimber M. A. , Martin A. D. , Ryskin M. G., Phys. Rev. D **63**, 114027, (2001), [arXiv:hep-ph/0101348]

KMR prescription to obtain unintegrated PDF from collinear one is based on the mechanism of last step parton k_T-dependent radiation and the assumption of strong angular ordering:

$$\Phi_q(x,k_T^2,\mu^2) = T_q(k_T,\mu)\frac{\alpha_s(k_T^2)}{2\pi}\int\limits_x^{1-\Delta} dz \int^{k_T^2} \frac{dq_T^2}{q_T^2} \times$$
$$\times \left[P_{qg}(z) f_g\left(\frac{x}{z},q_T^2\right) + P_{qq}(z) f_q\left(\frac{x}{z},q_T^2\right)\right].$$

Where $P_{qg}(z)$, $P_{qq}(z)$- DGLAP splitting functions, $T_q(k_T,\mu)$- Sudakov formfactor:

$$T_q(k_T,\mu) = exp\left\{-\int\limits_{k_T^2}^{\mu^2}\frac{dq_T^2}{q_T^2}\frac{\alpha_s(q_T^2)}{2\pi}\sum_{a'}\int\limits_0^{1-\Delta} P_{qa'}(z')dz'\right\}$$

where $\Delta = \frac{k_T}{\mu+k_T}$ ensures the *rapidity ordering of the last emission and particles produced in the hard subprocess.*

The photoproduction kinematics.

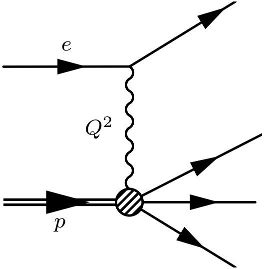

Photon carries the virtuality $q^2 = -Q^2$, and fraction of the electron's energy y (inelasticity). Photoproduiction kinematics is:

$$Q \ll yE_e$$

The photoproduction cross section can be calculated in the Weizsäcker-Williams approximation:

$$\sigma(ep \to e\gamma jX) = \int dy G_{\gamma/e}(y)\sigma(\gamma p \to \gamma jX),$$

where

$$G_{\gamma/e}(y) = \frac{\alpha}{2\pi}\left\{\frac{1+(1-y)^2}{y}\log\left(\frac{Q^2_{max}}{Q^2_{min}}\right) + \right.$$
$$\left. +2m_e^2 y\left(\frac{1}{Q^2_{min}} - \frac{1}{Q^2_{max}}\right)\right\},$$

and $Q^2_{min} = m_e^2 y^2/(1-y)$, and $Q_{max} = 1$ GeV for ZEUS and H1 detectors at DESY HERA.

Motivation of the present study.

The process under consideration was studied in the NLO CPM [M. Fontannaz *et. al.* 2004] and standard k_T-factorization [M. Malyshev *et. al.* 2013]. The problems of this approaches are:

- NLO CPM describes well the rapidity spectra, but observables related with the transverse momentum, like p_T spectra or azimuthal decorrelations are described worse.
- LO in k_T-factorization describes better the p_T-spectra, but has internal problems due to the absence of gauge invariance of amplitudes with off-shell quarks in the initial state. In PRA the amplitudes are gauge invariant, due to the gauge invariance of effective action and Reggeon fields.
- The (formally NNLO) process $\gamma g \to \gamma g$ is found to be numerically large in CPM due to large gluon luminosity at small x. Computation with LO CPM amplitude in the off-shell kinematics gives even further enhancement, but what the correct computation will show?

Subprocesses in the LO PRA.

The **direct** subprocesses are ($q_1^2 = -\mathbf{q}_{T1}^2 = -t_1$, $q_{2,3,4}^2 = 0$):

$$Q(q_1) + \gamma(q_2) \rightarrow q(q_3) + \gamma(q_4), \quad (1)$$

$$R(q_1) + \gamma(q_2) \rightarrow g(q_3) + \gamma(q_4), \quad (2)$$

where $Q(\bar{Q})$ is the Reggeized quark (antiquark), and R is the Reggeized gluon from the proton. The photon fragmentation into partons ($\gamma \rightarrow q\bar{q}$) is enhanced by DGLAP logarithms, also, the nonperturbative contribution is present ($\gamma \rightarrow \rho, \omega, ... \rightarrow q\bar{q}$), so, the **resolved** subprocesses should be taken into account:

$$R(q_1) + q\,[\gamma]\,(\tilde{q}_2) \rightarrow q(q_3) + \gamma(q_4), \quad (3)$$

$$Q(q_1) + \bar{q}\,[\gamma]\,(\tilde{q}_2) \rightarrow g(q_3) + \gamma(q_4), \quad (4)$$

$$Q(q_1) + g\,[\gamma]\,(\tilde{q}_2) \rightarrow q(q_3) + \gamma(q_4). \quad (5)$$

The subprocesses (4,5) are found to contribute less then 5% of the total cross section, so we will skip them.
Also we skip the contributions with the fragmrntation of the final parton into photon, since in the experiment, the strong isolation condition was applied to the photons.

The $Q\gamma \to q\gamma$ (Compton-direct) subprocess.

The relevant Feynman rules for reggeized quark and gluon interactions are:

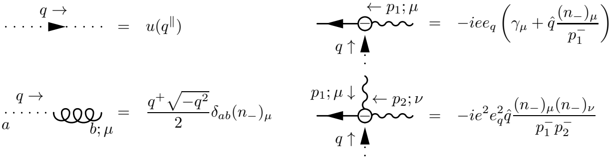

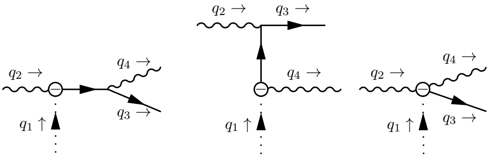

The squared amplitude is

$$\overline{|\mathcal{M}(Q\gamma \to q\gamma)|^2} = -32\pi^2\alpha^2 e_q^4 \frac{Sx_1}{b_4 su}\left(t_1 b_3^3 + s b_4^3 - u\right),$$

where the Sudakov variables are introduced: $a_{3,4} = 2q_2 q_{3,4}/S \sim q_{3,4}^+$, $b_{3,4} = 2P_1 q_{3,4}/S \sim q_{3,4}^-$, $S = 2P_1 q_2$.

The $Rq \to q\gamma$ (Compton-resolved) subprocess.

Here the Reggeized gluon comes from the proton ($\tilde{q}_2 = x_2 q_2$):

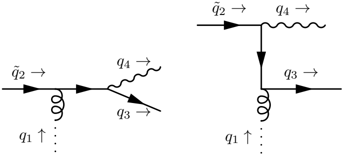

Squaring and averaging over initial state spins and colors we get:

$$\begin{aligned} \overline{|\mathcal{M}(Rq \to q\gamma)|^2} &= \frac{16}{3}\pi^2 \alpha \alpha_s e_q^2 \frac{S^2 x_1^2 x_2}{s t^2 t_1} \left\{ t \left[u b_3 + (t+u) b_4 - S a_3 b_3^2 + s x_2 \right] + \right. \\ &+ \left. S a_4 b_3 \left[s b_4 - t b_3 - (s+t) x_2 \right] \right\}. \end{aligned}$$

The collinear limit holds for both tree-level subprocesses.

The $R\gamma \to g\gamma$ (“box”) subprocess.

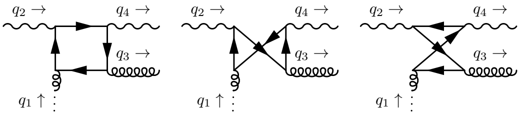

Three diagrams with the opposite direction of the fermion line are not shown. The helicity amplitude for the $(R\gamma \to g\gamma)$ subprocess is:

$$\mathcal{M}(R\lambda_2, \lambda_3\lambda_4) = -\frac{q_1^+}{2\sqrt{t_1}}(n_-)_{\mu_1}\varepsilon_{\mu_2}(1, -\lambda_2)\varepsilon^*_{\mu_3}(2, \lambda_3)\varepsilon^*_{\mu_4}(2, -\lambda_4)\mathcal{M}^{\mu_1\mu_2\mu_3\mu_4},$$

where $\lambda_i = \pm 1$. The polarization vectors are:$\varepsilon_\mu(j, \lambda) = \frac{1}{\sqrt{2}}\left[(n_x^{(j)})_\mu + i\lambda(n_y^{(j)})_\mu\right]$, where

$$n_x^{(1)} = \frac{1}{\Delta}((q_2q_3)q - (qq_3)q_2 - (qq_2)q_3),\ n_x^{(2)} = \frac{1}{\Delta}((q_3q_4)q - (qq_4)q_3 - (qq_3)q_4),$$

$$-(n_y^{(2)})^\mu = (n_y^{(1)})^\mu = n_y^\mu = \frac{1}{\Delta}\epsilon^{\mu q_2 q_3 q_4},\ \Delta = \frac{\sqrt{stu}}{2},\ q = q_2 + q_3.$$

The kinematical variables for the "box" subprocess.

Decompose the vector n^-:

$$n_- = \alpha n_+ + \beta_1 q_3 + \beta_2 q_4 + \gamma n_y.$$

And introduce two variables ($\gamma_{1,2}$):

$$\gamma_1 = \frac{q_4^+ \Delta}{\sqrt{t_1}} \gamma = \frac{u}{\sqrt{t_1}} |\mathbf{q}_{T3}||\mathbf{q}_{T4}| \sin(\phi), \; \gamma_2^2 = stu - \frac{(t+u)^2}{u^2} \gamma_1^2,$$

$$q_4^- q_4^+ = \frac{u}{(t+u)^2} \left[(u-t)(t_1 - t) - 2t^2 + \gamma_2 \sqrt{t_1} \right].$$

These variables has the simple collinear limits:

$$\gamma_1 \to 2\frac{u}{s} \Delta \sin(\phi_1), \; \gamma_2 \to 4\Delta \cos(\phi_1),$$

and lead to the simple and explicitly finite answer in the collinear limit.

The result for $R\gamma \to g\gamma$ amplitude.

$$\overline{|\mathcal{M}(\gamma + R \to \gamma + g)|^2} = \frac{\alpha^2\alpha_s^2}{4\pi^4}\left(\sum_q e_q^2\right)^2 \Big\{|\mathcal{M}(R+,++)|^2 + |\mathcal{M}(R+,+-)|^2 + + |\mathcal{M}(R+,-+)|^2 + |\mathcal{M}(R+,--)|^2\Big\},$$

$$\begin{aligned}
\mathcal{M}(R+,++) &= \mathcal{M}\left(t,u,t_1,\{f_i^{(1)}\},\mathcal{R}_1\right), \\
\mathcal{M}(R+,+-) &= \mathcal{M}\left(s,t,t_1,\{f_i^{(2)}\},\mathcal{R}_2\right), \\
\mathcal{M}(R+,-+) &= \mathcal{M}\left(s,u,t_1,\{f_i^{(3)}\},\mathcal{R}_3\right), \\
\mathcal{M}(R+,--) &= \frac{i\pi^2 4\sqrt{2}}{u\Delta}(t+u)\gamma_1,
\end{aligned}$$

The result for $R\gamma \to g\gamma$ amplitude.

$$\begin{aligned}\mathcal{M}\left(t,u,t_1,\{f_i\},\mathcal{R}\right) &= \frac{i\pi^2}{\sqrt{2}\Delta^3(t+u)}\left[f_1\left(B_0(t)-B_0(-t_1)\right)+f_2\left(B_0(u)-B_0(-t_1)\right)+\right.\\ &+ \left. f_3 E(t_1,t,u)+\mathcal{R}\right],\end{aligned}$$

where

$E(t_1,t,u) = tC_0(t)+uC_0(u)+(t+t_1)C_0(-t_1,t)+(u+t_1)C_0(-t_1,u)-tuD_0(-t_1,t,u)$.

Coefficient set 1:

$$\begin{aligned}
f_1^{(1)} &= \frac{-it^2}{2(t+t_1)^2}\left(2(s+2u)\left(t+t_1\right)\left(t+u\right)^2\gamma_1+4isu^2\left(2t\left(t+t_1\right)-ut_1\right)\sqrt{t_1}+\right.\\
&+ \left. u\left(s^2\left(s+t_1\right)+3su\left(s-t_1\right)+2u^2\left(s-t_1\right)\right)i\gamma_2\right),\\
f_2^{(1)} &= \frac{-itu}{2(u+t_1)^2}\left(2(s+2t)\left(u+t_1\right)\left(t+u\right)^2\gamma_1+4istu\left(tt_1-2u\left(u+t_1\right)\right)\sqrt{t_1}+\right.\\
&+ \left. u\left(s^3+s^2\left(3t+t_1\right)+st\left(2t-3t_1\right)-2t^2t_1\right)i\gamma_2\right),\\
f_3^{(1)} &= \frac{-i}{4s}\left(2(t+u)^2\left(t^2+t_1t+u\left(u+t_1\right)\right)\gamma_1+4istu^2(u-t)\sqrt{t_1}+\right.\\
&+ \left. u\left(t^3+t^2\left(u+t_1\right)+tu\left(u-2t_1\right)+u^2\left(u+t_1\right)\right)i\gamma_2\right),\\
\mathcal{R}_1 &= \frac{st^2u^2}{(t+t_1)(u+t_1)}\left((t_1-s)\gamma_2+2s(t-u)\sqrt{t_1}\right)
\end{aligned}$$

Coefficient sets 2,3.

$$
\begin{aligned}
f_1^{(2)} &= \frac{-is^2t}{2u}\left(2(t+u)(2t+u)\gamma_1 - 4itu^2\sqrt{t_1} - u(2t+u)i\gamma_2\right) \\
f_2^{(2)} &= \frac{ist^2}{2u(t+t_1)^2}\left(2(2s+u)\,(t+t_1)\,(t+u)^2\gamma_1 - 4isu^2\,(ut_1+t\,(t+t_1))\,\sqrt{t_1}\right. \\
&- \left. u\left(2\,(s+t_1)\,s^2+3su\,(s+t_1)+u^2\,(s-t_1)\right)i\gamma_2\right) \\
f_3^{(2)} &= \frac{is}{4u^2}\left(2\left(s^2+t_1s+t\,(t+t_1)\right)(t+u)^2\gamma_1 + 4ist^2u^2\sqrt{t_1}-\right. \\
&- \left. u\left(u^3+u^2\,(3t+t_1)+tu\,(4t+t_1)+2t^2\,(t+t_1)\right)i\gamma_2\right) \\
\mathcal{R}_2 &= -\frac{s^2t^2u}{t+t_1}\left(2u\sqrt{t_1}+\gamma_2\right)
\end{aligned}
$$

The coefficient set $\{f_i^{(3)}\},\mathcal{R}_3$ can be obtained from the set $\{f_i^{(2)}\},\mathcal{R}_2$ by the substitution:

$$
t \leftrightarrow u, \sqrt{t_1} \to -\sqrt{t_1}, \gamma_1 \to \gamma_1\frac{t}{u}, \qquad (6)
$$

which corresponds to the permutation of the final state particles.

Kinematical conditions.

The kinematical conditions for the prompt photon and jet associated production at DESY HERA. For all datasets, $Q^2_{max} = 1$ GeV^2, $E_e = 27.6$ GeV, and $E_p = 920$ GeV. Pseudorapidity $\eta = -\log\tan(\theta/2)$.

H1-2005	H1-2010
$0.2 < y < 0.7$	$0.1 < y < 0.7$
$E_T^{jet} > 4.5$ GeV	$E_T^{jet} > 4.5$ GeV
$5.0 < E_T^{\gamma} < 10.0$ GeV	$6.0 < E_T^{\gamma} < 15.0$ GeV
$-1.0 < \eta^{jet} < 2.3$	$-1.3 < \eta^{jet} < 2.3$
$-1.0 < \eta^{\gamma} < 0.9$	$-1.0 < \eta^{\gamma} < 2.4$

ZEUS-2007 I	ZEUS-2007 II
$0.2 < y < 0.8$	$0.2 < y < 0.8$
$6.0 < E_T^{jet} < 17.0$ GeV	$6.0 < E_T^{jet} < 17.0$ GeV
$5.0 < E_T^{\gamma} < 16.0$ GeV	$7.0 < E_T^{\gamma} < 16.0$ GeV
$-1.6 < \eta^{jet} < 2.4$	$-1.6 < \eta^{jet} < 2.4$
$-0.74 < \eta^{\gamma} < 1.1$	$-0.74 < \eta^{\gamma} < 1.1$

Expressions for differential cross sections.

Direct contributions:

$$\frac{d\sigma^{dir}}{dE_T^{jet}dE_T^{\gamma}d\eta^{jet}d\eta^{\gamma}d\phi} = \sum_{i=q,\bar{q},g} yG_{\gamma/e}(y)\Phi_i(x_1,t_1,\mu_F^2)\frac{\overline{|\mathcal{M}_{\gamma i}|^2}E_T^{jet}E_T^{\gamma}}{8\pi^2(Sx_1)^2},$$

where ϕ- azimuthal angle between $\mathbf{q}_T^{\gamma}$ and $\mathbf{q}_T^{jet}$.
Resolved contributions:

$$\frac{d\sigma^{res}}{dE_T^{jet}dE_T^{\gamma}d\eta^{jet}d\eta^{\gamma}d\phi dy} = \sum_{i,j=q,\bar{q},g} G_{\gamma/e}(y)\Phi_i(x_1,t_1,\mu_F^2)x_2 f_{j/\gamma}(x_2,\mu_F^2)\frac{\overline{|\mathcal{M}_{ij}|^2}E_T^{jet}E_T^{\gamma}}{8\pi^2(Sx_1x_2)^2},$$

where $f_{j/\gamma}(x_2,\mu_F^2)$- photon PDFs. Scale choice:

$$\mu_R = \mu_F = \xi \max(E_T^{\gamma}, E_T^{jet}),$$

and $1/2 < \xi < 2$ to obtain the scale uncertainty of the computation.

Numerical results for the “box” contribution.

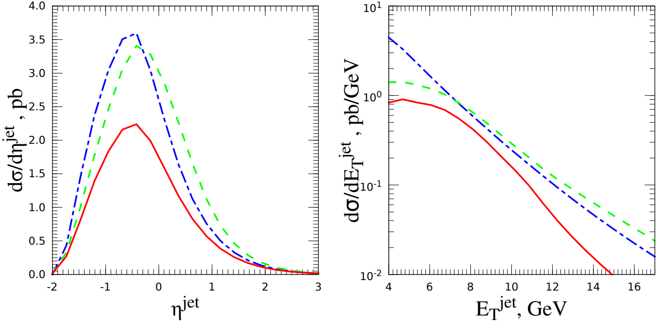

The exact cross-section for the box subprocess ($R\gamma \to g\gamma$) in the PRA (solid line) with H1-2005 kinematical conditions, and the cross section obtained integrating the CPM amplitude in off-shell kinematics (dashed line) are plotted together. The dash-dotted line corresponds to the CPM cross section for this subprocess, evaluated with the MRST-2006 LO gluon PDF. Left panel – η^{jet} spectrum, right panel – E_T^{jet} spectrum.

Photon and jet pseudorapidity distributions.

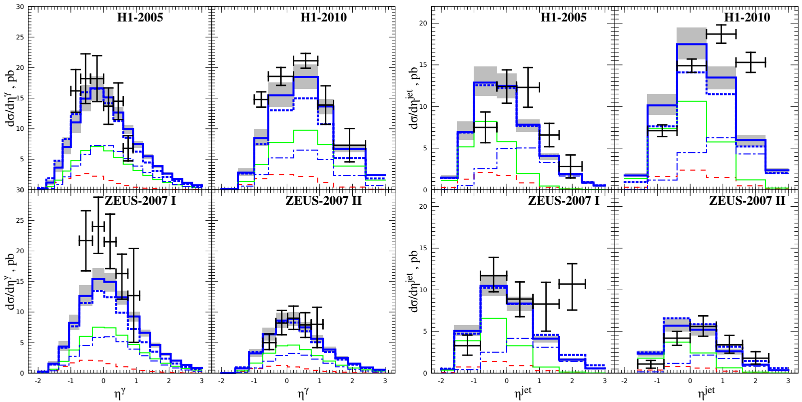

Prompt-photon pseudorapidity distributions in photoproduction, at DESY-HERA. **Thick solid** histogram – LO PRA prediction, thick dotted histogram – LO CPM prediction. Contributions to the LO PRA prediction is shown by the thin lines: $\gamma Q \to \gamma q$ – solid histogram, $\gamma R \to \gamma g$ – dashed histogram, $qR \to q\gamma$ – dash-dotted histogram.

Photon and jet transverse energy distributions.

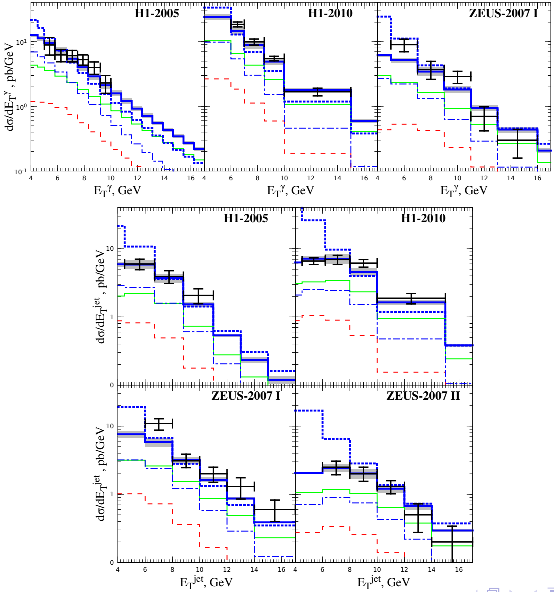

Parton momentum fractions.

ZEUS and H1 collaborations also presented the distributions of the data in variables:

$$x_p^{LO} = \frac{E_T^\gamma}{2E_p}\left(e^{\eta^{jet}} + e^{\eta^\gamma}\right), \quad x_\gamma^{LO} = \frac{E_T^\gamma}{2yE_e}\left(e^{-\eta^{jet}} + e^{-\eta^\gamma}\right),$$

$$x_\gamma^{obs} = \frac{1}{2yE_e}\left(E_T^{jet} e^{-\eta^{jet}} + E_T^\gamma e^{-\eta^\gamma}\right)$$

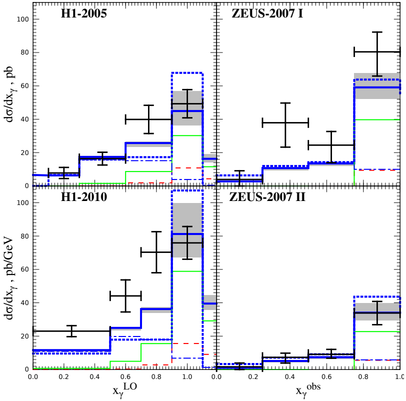

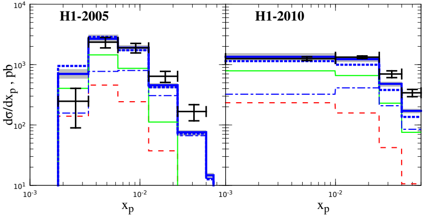

Azimuthal decorrelation observables.

Photon transverse momentum fraction ortohonal to the jet direction:

$$p_{\perp} = E_T^{\gamma} \sin(\phi)$$

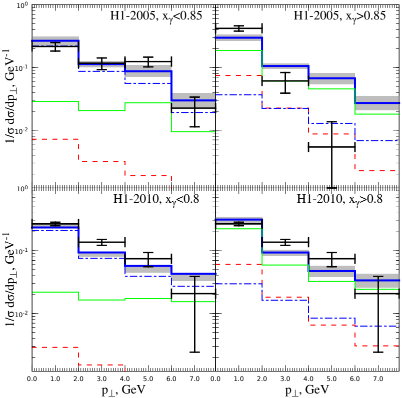

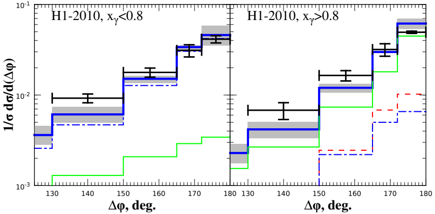

ZEUS-2013 data.

Kinematical conditions:

ZEUS-2013
$0.2 < y < 0.7$
$4.0 < E_T^{jet} < 35.0$ GeV
$6.0 < E_T^{\gamma} < 15.0$ GeV
$-1.5 < \eta^{jet} < 1.8$
$-0.7 < \eta^{\gamma} < 0.9$

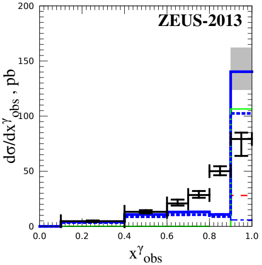

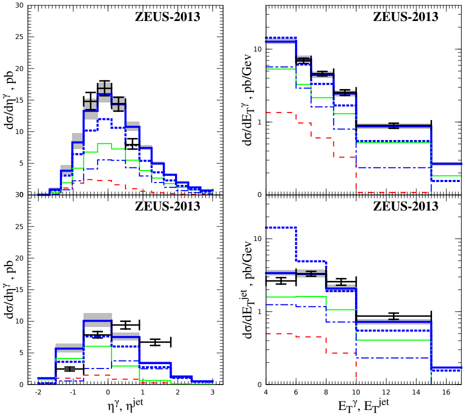

In the LO PRA, **direct** distribution is $\sim \delta(x_{obs}^{\gamma} - 1)$. Only $2 \to 3$ processes can smear the x_{γ}^{obs} distribution.

Conclusions.

- LO PRA gives in general good description of existing data on the photon associated with jet photoproduction. Quality of the description is comparable with NLO CPM.
- The "box" contribution is found to be sizable, but the space-like virtuality of the incoming parton *suppresses* it in comparison with LO CPM. It may indicate the better convergence of perturbative series in PRA.

Thank you for your attention!

Backup slides

Pseudorapidity distributions. Comparison with the NLO CPM.

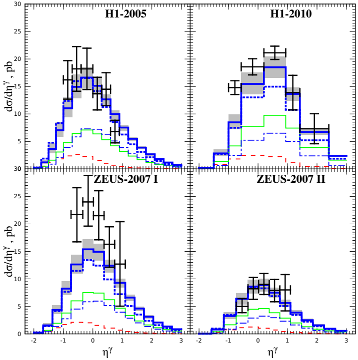

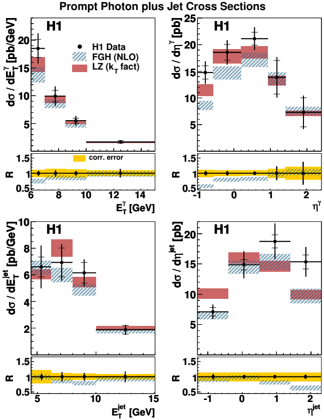

Prompt-photon pseudorapidity distributions in photoproduction, at DESY-HERA. **Thick solid** histogram – LO PRA prediction, thick dotted histogram – LO CPM prediction. Contributions to the LO PRA prediction is shown by the thin lines: $\gamma Q \to \gamma q$ – solid histogram, $\gamma R \to \gamma g$ – dashed histogram, $qR \to q\gamma$ – dash-dotted histogram. Plot on the right panel is taken from [Eur. Phys. J. C**66**, 17].

Pseudorapidity distributions. Comparison with the NLO CPM.

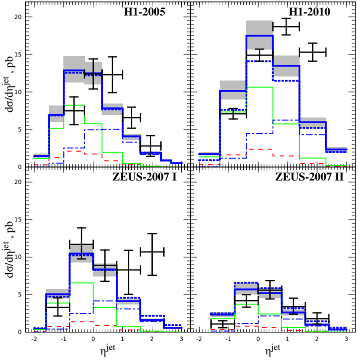

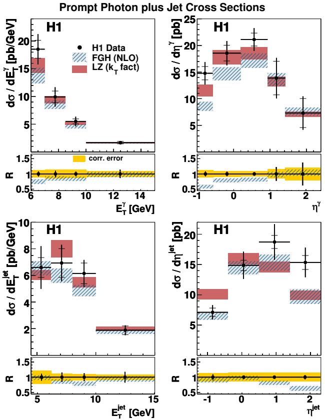

Jet pseudorapidity distributions in photoproduction, at DESY HERA.

Transverse energy distributions.

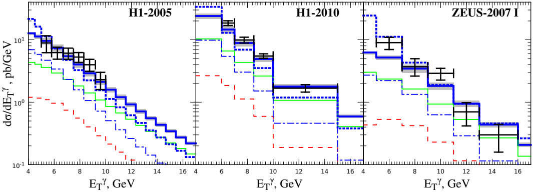

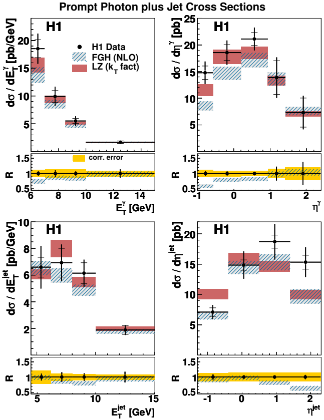

Prompt-photon E_T distributions in photoproduction, at DESY HERA.

Transverse energy distributions.

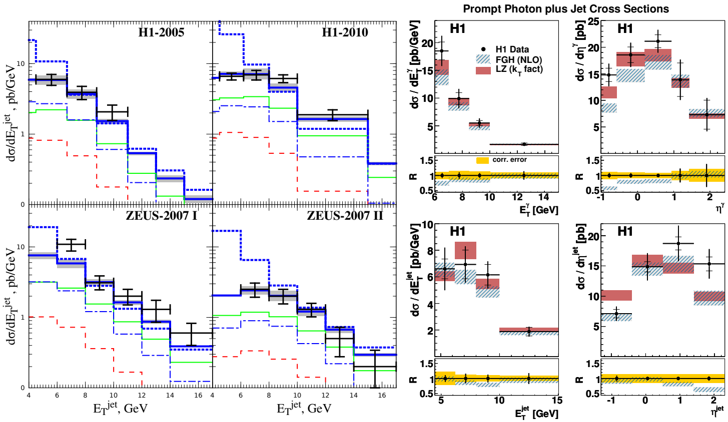

Prompt-photon E_T distributions in photoproduction, at DESY HERA.

Parton momentum fractions.

The x_γ-spectra:

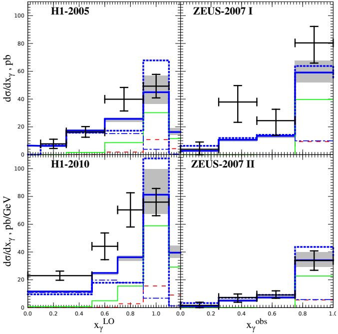

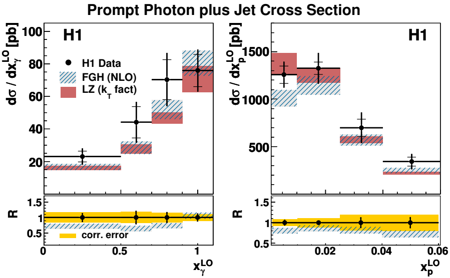

Plot on the right panel is taken from [Eur. Phys. J. C**66**, 17].

Azimuthal decorrelation observables.

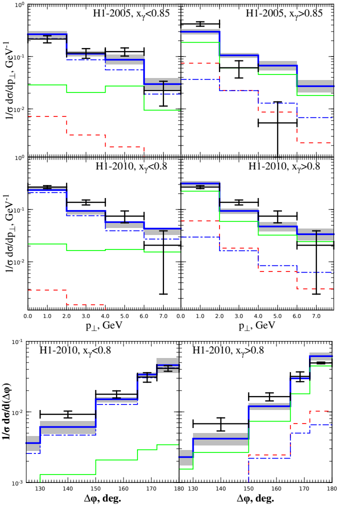

Photon momentum fraction ortohonal to the jet direction:

$$P_T = E_T^{\gamma} \sin(\phi)$$

Plot from [Eur. Phys. J. C**66**, 17]: